mathematics

MDPI

Article

Solving SIVPs of Lane–Emden–Fowler Type Using a Pair of Optimized Nyström Methods with a Variable Step Size

Mufutau Ajani Rufai [1,*] and Higinio Ramos [2,3]

1 Department of Mathematics, University of Bari Aldo Moro, 70125 Bari, Italy
2 Scientific Computing Group, Universidad de Salamanca, Plaza de la Merced, 37008 Salamanca, Spain
3 Escuela Politécnica Superior de Zamora, Campus Viriato, 49022 Zamora, Spain
* Correspondence: mufutau.rufai@uniba.it

Abstract: This research article introduces an efficient method for integrating Lane–Emden–Fowler equations of second-order singular initial value problems (SIVPs) using a pair of hybrid block methods with a variable step-size mode. The method pairs an optimized Nyström technique with a set of formulas applied at the initial step to circumvent the singularity at the beginning of the interval. The variable step-size formulation is implemented using an embedded-type approach, resulting in an efficient technique that outperforms its counterpart methods that used fixed step-size implementation. The numerical simulations confirm the better performance of the variable step-size implementation.

Keywords: hybrid block technique; Lane–Emden–Fowler problems; optimization strategy; starting procedure; adaptive formulation

MSC: 65L05; 65L06; 65L20

check for updates

Citation: Rufai, M.A.; Ramos, H. Solving SIVPs of Lane–Emden–Fowler Type Using a Pair of Optimized Nyström Methods with a Variable Step Size. *Mathematics* **2023**, *11*, 1535. https://doi.org/10.3390/math11061535

Academic Editors: Patricia J. Y. Wong and Luigi Rodino

Received: 10 February 2023
Revised: 15 March 2023
Accepted: 20 March 2023
Published: 22 March 2023

1. Introduction

The goal of this research paper was to find a reliable numerical approach for solving second-order SIVPs Lane–Emden–Fowler equations of the form:

$$q''(x) + \frac{\lambda}{x} q'(x) = w(x, q(x)),\ q(x_0) = q_0,\ q'(x_0) = q'_0, x_0 = 0 \le x \le x_N, \tag{1}$$

where $\lambda \ge 1$, q_0, q'_0 are real numbers; x_0 and x_N represent the initial and final points of the integration interval, respectively; and $w(x, q(x))$ is a continuous real function. We note that the necessary conditions for the existence and uniqueness of the solution to problem (1) were established in [1,2].

Equations of the form (1) are commonly encountered in many fields, such as astrophysics, mathematical modeling, celestial mechanics, physical and social sciences, and engineering. These types of equations have also been used to model various systems, including chemical reactors, thermal behavior of gas spheres, reaction–diffusion processes in porous catalysts, stellar structure, isothermal gas spheres, and thermionic current theory (as cited in sources such as [3–7], etc.).

The problem under consideration becomes one of the most complex problems to integrate analytically, due to the nonlinear properties of the second order SIVP and the singularity at $x = 0$. Therefore, numerical methods are essential for providing an approximate and reasonable solution.

Many scholars have extensively investigated the model in (1) and similar problems and have developed various methods for solving them. These methods include the implicit Euler method, various types of spline methods, the homotopy-perturbation technique, the variational iteration techniques, the Adomian decomposition method, a Padè approximation method, various types of collocation methods, finite difference methods, the heuristics approach, the differential transform method, the pseudospectral method, Taylor wavelet techniques, hybrid block methods, Nyström methods, the Haar wavelet resolution technique, iterative methods, spectral methods, Jacobi–Gauss collocation techniques, or asymptotic numerical strategies (see [8–25]).

In this study, we aimed to obtain a variable step-size formulation of a pair of optimized Nyström methods (PONMs) developed in [14] to further improve their performance. The main formulas of the existing PONM are given as follows:

$$
\begin{aligned}
q_{n+1} &= q_n + hq_n' + \frac{1}{360}h^2\left(18w_n + 7\left(\sqrt{21}+7\right)w_{n+r} + 64w_{n+s} - 7\left(\sqrt{21}-7\right)w_{n+t}\right), \\
q_{n+1}' &= q_n' + h\left(\frac{1}{20}w_n + \frac{49}{180}w_{n+r} + \frac{16}{45}w_{n+s} + \frac{49}{180}w_{n+t} + \frac{1}{20}w_{n+1}\right),
\end{aligned} \tag{2}
$$

while the additional formulas to avoid the singularity of the existing PONM are given by

$$
\begin{aligned}
q_1 &= q_0 + hq_0' \\
&\quad + h^2(0.2009319137389590w_{\bar r} + 0.2292411063595862w_{\bar s} + 0.0698269799014541w_{\bar t}), \\
q_1' &= q_0' + h(0.2204622111767684w_{\bar r} + 0.3881934688431719w_{\bar s} \\
&\qquad + 0.3288443199800597w_{\bar t} + 0.0625w_1),
\end{aligned} \tag{3}
$$

with

$$
r = \frac{\left(7-\sqrt{21}\right)}{14}, \quad s = \frac{1}{2}, \quad t = \frac{\left(7+\sqrt{21}\right)}{14}, \quad \bar r \simeq 0.0885879595127039,
$$

$$
\bar s \simeq 0.4094668644407347, \quad \bar t \simeq 0.7876594617608470.
$$

Note that the formulas in (3) do not use the value w_0, thus obtaining an approximate value for $q(x_1)$. After the formulas in (3) and the others needed for the block formulation are applied in the first subinterval, the formulas in (2) and the corresponding ones to form the main block method are applied in the subsequent subintervals. The reader is referred to Equations (10) and (14) in reference [14] to see the remaining formulas, including the complete description and theoretical analysis of the PONM method.

We remark that the main novelty of this study is a reasonable error estimation and the variable step-size implementation using embedded type approaches, which allowed us to very efficiently solve problems of the form in (1) when large integration intervals are considered.

2. Error Estimation and Mesh Selection of the PONMs

Using a fixed step-size scheme to solve a SIVP may be unreasonable because the solution rapidly changes within the integration interval. To improve efficiency, the PONM should be implemented with variable step sizes. This can be achieved by using a lower-order technique (LOT) to compute the local error at the end-point on each subinterval $[x_n, x_{n+1}]$. In this article, an embedding approach is utilized to formulate the suggested technique in variable step-size mode; this means that in addition to the approximation provided by q_{n+1}, an additional LOT approximation given by q_{n+1}^* is still needed. The difference between q_{n+1} and q_{n+1}^* enables us to estimate the local error. A fourth-order multistep formula, given by the following Equation (4),

$$
q_{n+1}^* = \frac{1}{6}\left(3-\sqrt{21}\right)q_{n+r} + \frac{1}{6}\left(\sqrt{21}+3\right)q_{n+t} - \frac{1}{42}h^2\left(\left(\sqrt{21}-5\right)w_{n+r} - 8w_{n+s} - \left(\sqrt{21}+5\right)w_{n+t}\right), \tag{4}
$$

was used to estimate the local error at the end point, with a local truncation error of $\frac{h^6 q^{(6)}(x_n)}{987840} + O(h^7)$.

By following a similar strategy as the one reported in [16], the steps listed below are taken in order to increase the efficiency of the PONMs:

- Equations (2) and (3) and those in Equations (10) and (14) from [14] are used simultaneously at x_{n+1}, using the known solution at x_n.
- We use the multistep formula in (4) to find a second approximation to the solution of the problem under consideration at the grid point x_{n+1}.
- We estimate the local error using the following formula

$$ESTM = \|q_{n+1} - q^*_{n+1}\|,$$

where q^*_{n+1} and q_{n+1} are the values obtained by the fourth-order multistep formula in (4) and the PONM in (2) and (3) together with Equations (10) and (14) from [14], respectively.

Given a user-defined tolerance, ABTOL, we proceed as follows:

- If ESTM $\leq$ ABTOL, the results are accepted, and the step size is increased to $h_{new} = 2 \times h_{old}$.
- If ESTM $>$ ABTOL, the results are rejected, and the calculations are repeated with a new step size given by

$$h_{new} = \mu \times h_{old} \left(\frac{ABTOL}{|ESTM|} \right)^{1/(lo+2)}, \tag{5}$$

where $0 < \mu < 1$ is an adjustment factor to prevent failed steps, and $lo = 4$ is the order of the LOT. For more details about the choice of the variable step size strategy in (5), see [21,22].

3. Computational Details

The PONM is executed utilizing the error estimation and the mesh selection strategy presented in Section 2. The proposed PONM is written as $\boldsymbol{W}(\boldsymbol{u}) = \boldsymbol{0}$, and the unknowns are expressed as

$$\tilde{\mathbf{Q}} = \{q_{\bar{r}}, q_{\bar{s}}, q_{\bar{t}}, q'_{\bar{r}}, q'_{\bar{s}}, q'_{\bar{t}}\} \bigcup \{q_i\}_{i=1,2,\ldots,N} \bigcup \{q'_i\}_{i=1,\ldots,N} \bigcup \{q_{i+r}, q_{i+s}, q_{i+t}, q'_{i+r}, q'_{i+s}, q'_{i+t}\}_{i=1,2,\ldots,N-1}.$$

We use the modified Newton's method (MNM) to solve the nonlinear systems, with a stopping criterion of 100 maximum iterations and an error from 2 subsequent estimates provided by $\|\tilde{\mathbf{Q}}^{\mathbf{i+1}} - \tilde{\mathbf{Q}}^{\mathbf{i}}\| \leq \mathbf{10^{-16}}$. We write MNM as

$$\tilde{\mathbf{Q}}^{\mathbf{i+1}} = \tilde{\mathbf{Q}}^{\mathbf{i}} - (\mathbf{J_0})^{-\mathbf{1}} \mathbf{W}^{\mathbf{i}},$$

where $\tilde{\mathbf{Q}}^{\mathbf{i+1}}$ is the updated estimate of the solution at iteration $i+1$, $\tilde{\mathbf{Q}}^{\mathbf{i}}$ is the current estimate of the solution at iteration i, $\mathbf{J_0}$ is the frozen Jacobian matrix of the function $\mathbf{W}$ at the current estimate $\tilde{\mathbf{Q}}^{\mathbf{i}}$, and $\mathbf{W}^i$ is the vector of residuals at the current estimate $\tilde{\mathbf{Q}}^{\mathbf{i}}$. The following initializing values were used with MNM for each iteration:

$$\begin{aligned}
&q_j = q_0 + (jh_0)q'_0, \quad q'_j = q'_0, \quad j = \bar{r}, \bar{s}, \bar{t}, 1,\\
&q_{n+j} = q_n + (jh)q'_n + \frac{(jh)^2}{2} w_n, \quad q'_{n+j} = q'_n + (jh)w_n, \quad n = 1, 2, \ldots, N-1, \; j = r, s, t, 1.
\end{aligned}$$

4. Numerical Experiments

In this part, we give the numerical results for the proposed PONM on different SIVPs of the form (1). We point out that the estimation and mesh selection technique described in Section 2, as well as the PONM method given in (2) and (3) and the remaining formulas presented in Equations (10) and (14) in [14], play a crucial role in determining the efficiency of the proposed method. The PONM was implemented in Mathematica 11.0 by using the constructed codes. We utilized a PC with an i7 processor, 16 GB of RAM, and the 64-bit Windows 10 operating system. To measure the accuracy of our results, we use the Maximum Absolute Error (MAE) formula, which is defined as:

$$MAE = \max_{j=0,\ldots,N} \left\{ \|q(x_j) - q_j\|_\infty \right\},$$

In the above equation, $q(x_j)$ represents the exact solution, and q_j represents the computed result at each point x_j on the discrete grid.

In the tables and figures, the following acronyms are used:

- PONM: The pair optimized hybrid Nyström method whose main formulas are given in (2) and (3).
- HPM : The homotopy perturbation method in [23].
- WNT: The wavelet based neural technique in [25].
- NM: The Nyström method in [26].
- BVM: The boundary value method in [27]
- NS : Number of steps.
- TFE : Total number of function evaluations.
- ABTOL : Absolute tolerance.
- CPU : Computational cost in seconds.

4.1. Problem One

We consider the SIVP from [27],

$$q''(x) + \frac{2}{x} q'(x) + q(x)^5 = 0, \quad q(0) = 1, q'(0) = 0, \quad x \in [x_0, x_N], \tag{6}$$

with exact solution $q(x) = \left(1 + \frac{x^2}{3}\right)^{-\frac{1}{2}}$.

The results in Tables 1 and 2 demonstrate the accuracy of the PONM in terms of MAE. Additionally, the comparison of the PONM and the exact solutions for (6) with ABTOL $= 10^{-6}, h_{ini} = 10^{-3}, x \in [0, 500]$ in Figure 1, shows that the PONM technique in variable step-size implementation strongly fits the analytical solution.

Table 1. Comparison of the numerical results on Problem 6 with $x \in [0, 1]$.

ABTOL	Method	NS	MAE
10^{-4}	PONM	3	2.7228×10^{-7}
	HPM	4	7.8000×10^{-4}
	WNT	4	5.9000×10^{-6}
10^{-6}	PONM	4	8.7887×10^{-9}
	HPM	5	2.4000×10^{-6}
	WNT	5	3.4000×10^{-7}

Table 2. Numerical results for (6) with $h_0 = 10^{-3}, x \in [0, 500]$.

ABTOL	Method	NS	TFE	CPU	MAE
10^{-4}	PONM	57	284	0.0956	5.6646×10^{-5}
	NM	58	289	0.1047	1.2890×10^{-5}
10^{-6}	NM	61	304	0.1132	6.5525×10^{-8}
	NM	64	319	0.1338	1.6384×10^{-7}
10^{-8}	PONM	72	359	0.1515	3.3750×10^{-10}
	NM	80	399	0.1867	2.2762×10^{-5}

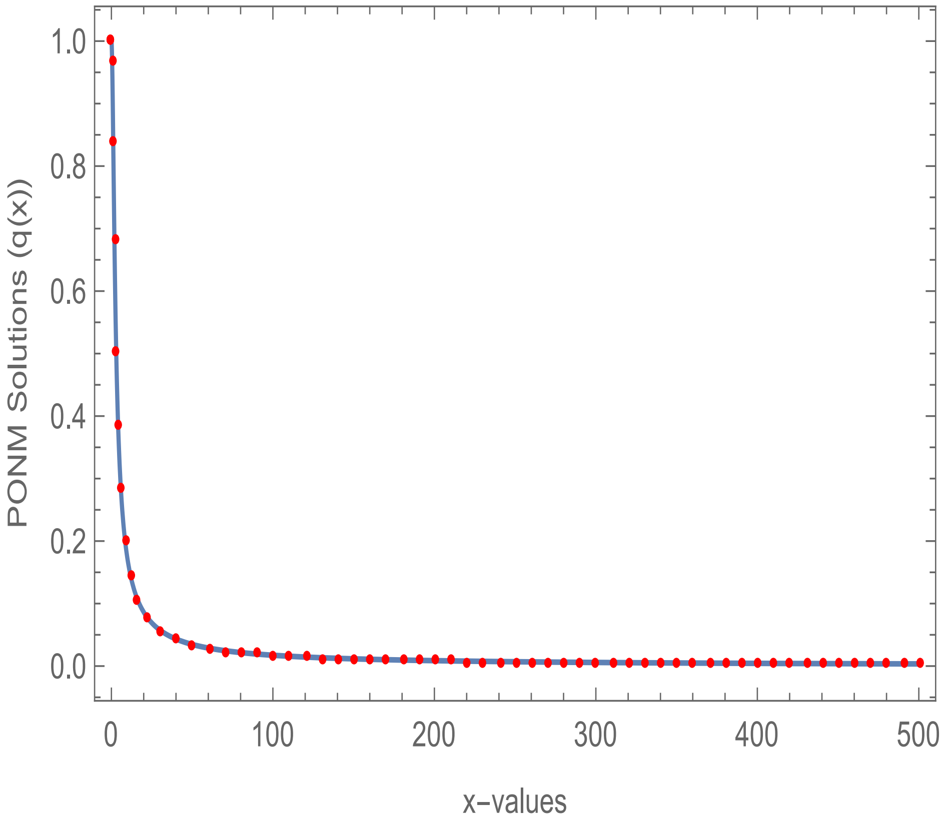

Figure 1. Comparison of PONM and the exact solution for (6).

4.2. Problem Two

We consider

$$q''(x) = -\frac{2}{x}q'(x) - 9\cos(3x) - \frac{6}{x}\sin(3x), \quad q(0) = 2, q'(0) = 0, \quad x \in [x_0, x_N], \tag{7}$$

with exact solution $q(x) = 1 + \cos(3x)$.

From the data reported in Tables 3 and 4, the proposed PONM outperforms the BVM and NM methods in terms of MAE, TFE, and CPU. Additionally, the comparison of PONM and the exact solution for (7) with ABTOL = $10^{-7}, h_{ini} = 10^{-2}, x \in [0, 80\pi]$ in Figure 2, shows that the PONM method with a variable step size fits the exact solution.

Table 3. Comparison of the numerical results for Problem 6 with $x \in [0, 2\pi]$.

ABTOL	Method	NS	MAE
10^{-6}	PONM	22	1.6792×10^{-8}
	BVM	40	1.5067×10^{-5}
10^{-8}	PONM	43	3.0682×10^{-11}
	BVM	80	2.2747×10^{-7}
10^{-10}	PONM	88	1.0991×10^{-13}
	BVM	160	3.5299×10^{-9}

Table 4. Numerical results for (6) with $h_0 = 10^{-3}, x \in [0, 60\pi]$.

ABTOL	Method	NS	TFE	CPU	MAE
10^{-5}	PONM	397	1984	0.7901	5.7799×10^{-6}
	NM	577	2884	0.9730	5.2609×10^{-5}
10^{-7}	PONM	843	4214	1.4590	6.7684×10^{-10}
	NM	1209	6044	1.7620	1.7594×10^{-7}
10^{-9}	PONM	1772	8859	2.9444	9.4920×10^{-11}
	NM	2541	12704	3.5005	7.2988×10^{-10}

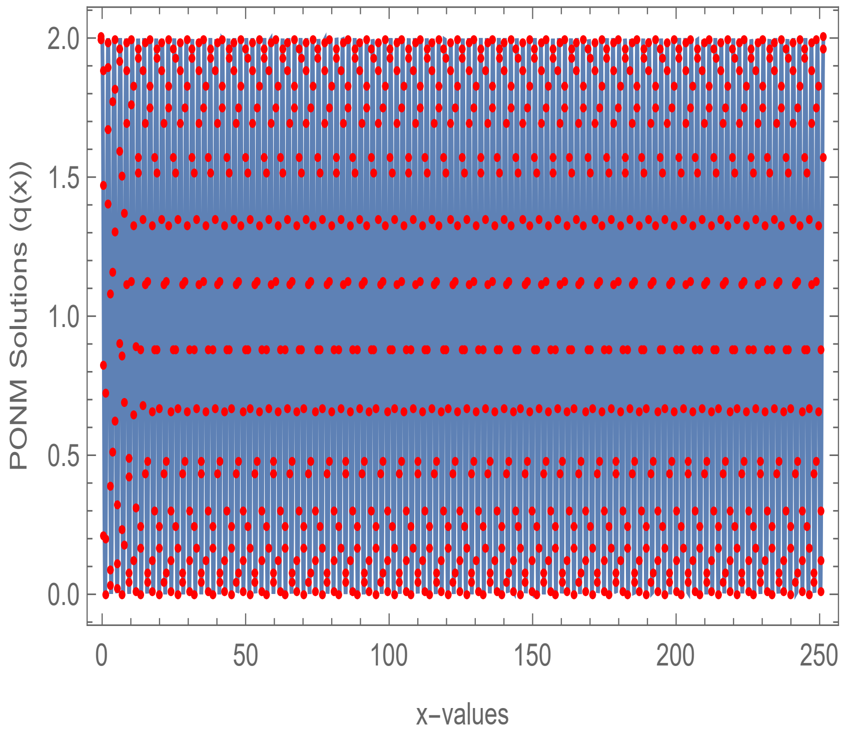

Figure 2. Comparison of PONM and the exact solution for (7).

4.3. Problem Three

For the last problem in this research, we applied the proposed method to the following system of SIVP from [26],

$$q_1''(x) + \frac{1}{x}q_1'(x) - q_2^3(x)\left(q_1^2(x) + 1\right) = 0,$$
$$q_2''(x) + \frac{3}{x}q_2'(x) - q_2^5(x)\left(q_1^2(x) + 3\right) = 0, \quad x \in [x_0, x_N], \tag{8}$$

with initial values

$$q_1(0) = 1, \quad q_1'(0) = 1,$$
$$q_2(0) = 0, \quad q_2'(0) = 0,$$

and the true solution from [26] is

$$q_1(x) = \sqrt{x^2+1}, \qquad q_2(x) = \frac{1}{\sqrt{x^2+1}}.$$

The suggested PONM surpasses the NM method in terms of MAE, TFE, and CPU, according to the data in Table 5. Furthermore, the comparison of PONM and the exact solution for (8) with ABTOL = $10^{-10}, h_{ini} = 10^{-3}, x \in [0, 200]$, is shown in Figure 3; one can see that the PONM fits the exact solution.

Table 5. Numerical results on (8) with $h_0 = 10^{-3}, x \in [0, 100]$.

ABTOL	Method	NS	FE	CPU	MAE
10^{-8}	PONM	40	199	0.4023	2.2212×10^{-8}
	NM	43	214	0.4487	3.0775×10^{-6}
10^{-7}	PONM	55	274	0.5315	1.2844×10^{-9}
	NM	59	294	0.6269	3.1063×10^{-7}
10^{-9}	PONM	78	389	0.7272	4.8580×10^{-11}
	NM	82	409	0.8463	3.3702×10^{-8}

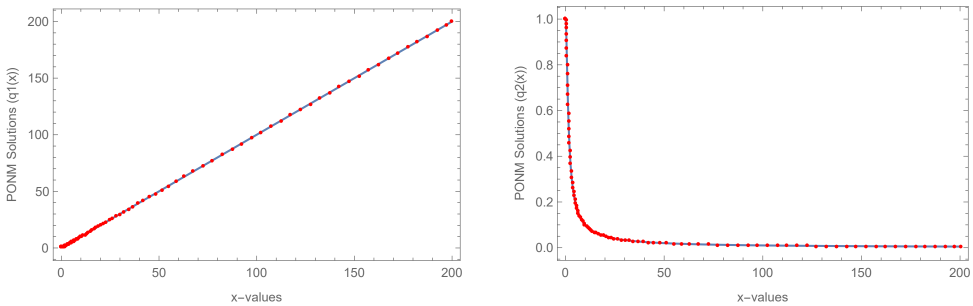

Figure 3. Comparison of PONM and exact for (8).

5. Conclusions

In this paper, we introduced and applied a variable step-size version of a pair of optimized Nyström methods (PONM) to give numerical solutions to Lane–Emden–Fowler equations of second-order singular initial value problems. The error estimation and mesh selection of the PONM were discussed. Two scalar examples and a system of numerical experiments revealed that the variable step-size formulation using an embedded-type approach results in an efficient technique that outperforms its counterpart methods that use fixed step-size implementation. The type of strategy presented in this paper could be considered for solving time-dependent partial differential equations and fractional-order differential equations of the Lane–Emden–Fowler type in future research work.

Author Contributions: Conceptualization, M.A.R. and H.R.; Methodology, M.A.R.; Software, M.A.R.; Validation, H.R.; Formal analysis, M.A.R. and H.R.; Writing—original draft, M.A.R.; Writing—review & editing, M.A.R. and H.R.; Visualization, H.R.; Supervision, H.R.; Funding acquisition, H.R. All authors have read and agreed to the published version of the manuscript.

Funding: This research received no external funding.

Data Availability Statement: Not applicable.

Conflicts of Interest: The authors declare that there is no conflict of interest.

References

1. Agarwal, R.P.; O'Regan, D. Second order initial value problems of Lane-Emden type. *Appl. Math. Lett.* **2007**, *20*, 1198–1205. [CrossRef]
2. Biles, D.C.; Robinson, M.P.; Spraker, J.S. A generalization of the Lane-Emden equation. *J. Math. Anal. Appl.* **2002**, *273*, 654–666. [CrossRef]
3. Chandrasekhar, S. *Introduction to Study of Stellar Structure*; Dover: New York, NY, USA, 1967.
4. Rufai, M.A.; Ramos, H. Numerical integration of third-order singular boundary-value problems of Emden–Fowler type using hybrid block techniques. *Commun. Nonlinear Sci. Numer. Simul.* **2022**, *105*, 106069. [CrossRef]
5. Rufai, M.A.; Ramos, H. Solving third-order Lane–Emden–Fowler equations using a variable step-size formulation of a pair of block methods. *J. Comput. Appl. Math.* **2023**, *420*, 114776. [CrossRef]
6. Rufai, M.A.; Ramos, H. Numerical Solution for Singular Boundary Value Problems Using a Pair of Hybrid Nyström Techniques. *Axioms* **2021**, *10*, 202. [CrossRef]
7. Shawagfeh, N.T. Nonperturbative approximate solution for Lane-Emden equation. *J. Math. Phys.* **1993**, *34*, 4364–4369. [CrossRef]
8. Koch, O.; Kofler, P.; Weinmüller, E.B. The implicit Euler method for the numerical solution of singular initial value problems. *Appl. Numer. Math.* **2000**, *34*, 231–252. [CrossRef]
9. Chowdhury, M.S.H.; Hashim, I. Solution of a class of singular second-order IVPs by homotopy-perturbation method. *Phys. Lett. A* **2007**, *365*, 439–447. [CrossRef]
10. Mehrpouya, M.A. An efficient pseudospectral method for numerical solution of nonlinear singular initial and boundary value problems arising in astrophysics. *Math. Methods Appl. Sci.* **2016**, *39*, 3204–3214. [CrossRef]
11. Bhrawy, A.H.; Alofi, A.S. A Jacobi-Gauss collocation method for solving nonlinear Lane-Emden type equations. *Commun. Nonlinear Sci. Numer. Simul.* **2012**, *17*, 62–70. [CrossRef]
12. Swati; Singh, K.; Verma, A.K.; Singh, M. Higher order Emden–Fowler type equations via uniform Haar Wavelet resolution technique. *J. Comput. Appl. Math.* **2020**, *376*, 112836. . [CrossRef]
13. Sabir, Z.; Raja, M.A.Z.; Umar, M. Design of neuro-swarming-based heuristics to solve the third-order nonlinear multi-singular Emden–Fowler equation. *Eur. Phys. J. Plus* **2020**, *135*, 410. [CrossRef]
14. Rufai, M.A.; Ramos, H. Numerical solution of second-order singular problems arising in astrophysics by combining a pair of one-step hybrid block Nyström methods. *Astrophys. Space Sci.* **2020**, *365*, 96. [CrossRef]
15. Singh, R.; Kumar, J. The Adomian decomposition method with Green's function for solving nonlinear singular boundary value problems. *J. Appl. Math. Comput.* **2014**, *44*, 397–416. [CrossRef]
16. Rufai, M.A.; Ramos, H. A variable step-size fourth-derivative hybrid block strategy for integrating third-order IVPs, with applications. *Int. J. Comput. Math.* **2022**, *99*, 292–308. [CrossRef]
17. Heydari, M.; Hosseini, S.M.; Loghmani, G.B. Numerical solution of singular IVPs of Lane-Emden type using integral operator and radial basis functions. *Int. J. Ind. Math.* **2012**, *4*, 135–146.
18. Dong, Q.L. A new iterative method with alternated inertia for the split feasibility problem. *J. Nonlinear Var. Anal.* **2021**, *5*, 939–950.
19. Zhang, J.; Shen, Y.; He, J. Some analytical methods for singular boundary value problem in a fractal space: A review. *Appl. Comput. Math.* **2019**, *18*, 225–235.
20. Ascher, U.M.; Petzold, L.R. *Computer Methods for Ordinary Differential Equations and Differential-Algebraic Equations*; Society for Industrial and Applied Mathematics (SIAM): Philadelphia, PA, USA, 1998.
21. Shampine, L.F.; Gordon, M.K. *Computer Solutions of Ordinary Differential Equations: The Initial Value Problem*; Freeman: San Francisco, CA, USA, 1975.
22. Stoer, J.; Bulirsch, R. *Introduction to Numerical Analysis*; Springer: Berlin/Heidelberg, Germany, 2002.
23. Yıldırım, A.; Özis, T. Solutions of singular IVPs of Lane-Emden type by homotopy perturbation method. *Phys. Lett. A* **2007**, *369*, 70–76. [CrossRef]
24. Chawla, M.M.; Jain, M.K.; Subramanian, R. The application of explicit Nyström methods to singular second order differential equations. *Comput. Math. Appl.* **1990**, *19*, 47–51. [CrossRef]
25. Rahimkhani, P.; Ordokhani, Y. Orthonormal Bernoulli wavelets neural network method and its application in astrophysics. *Comp. Appl. Math.* **2021**, *40*, 78. [CrossRef]
26. Ramos, H.; Rufai, M.A.; An adaptive pair of one-step hybrid block Nyström methods for singular initial-value problems of Lane–Emden–Fowler type. *Math. Comput. Simul.* **2022**, *193*, 497–508. [CrossRef]
27. Wang, H.; Zhang, C. The adapted block boundary value methods for singular initial value problems. *Calcolo* **2018**, *55*, 22. [CrossRef]